indicated that a small amount of crystal deterioration had occurred during the course of data collection. The intensities of this set of standards had decreased by an average value of 8.5% at the end of the data collection. Data reduction, including correction for crystal decay, and all further calculations were done with the TEXSAN package of crystallographic programs.[24]

The structure was solved with the direct-methods program MITHRIL,[25] where all of the non-hydrogen atoms were located on an electron density map. Most of the hydrogen atoms were located on a difference electron density map after the anisotropic stage had been reached. The hydrogen atoms were subsequently added to the model as fixed contributions at calculated positions with the assumptions C–H = 0.98 Å and $B_H = 1.2B_{eq}$ (attached carbon atom). The methyl hydrogen atoms were idealized to sp^3 geometry based on their locations in the difference electron density map. The final refinement cycle for the 1332 intensities with $F_o^2 > 3\sigma(F_o^2)$ and the 181 variables (anisotropic non-hydrogen atoms and hydrogen atoms fixed) gave agreement indices of $R = 0.048$ and $R_w = 0.052$. The final difference electron density map contained maximum and minimum peak heights of 0.16 and −0.19 e/Å^3. Scattering factors were obtained from the usual sources.[26]

X-ray Crystallographic Analysis of 53. Crystals of **53** are clear and colorless with a rodlike habit. Examination of the diffraction pattern on a Rigaku AFC5 diffractometer indicated a monoclinic crystal system with systematic absences $0k0$, $k = 2n + 1$. Since two molecules in the unit cell result in a reasonable calculated density, the space group is assumed to be $P2_1$. At room temperature, the cell constants $a = 5.811$ (1) Å, $b = 17.310$ (2) Å, $c = 8.731$ (1) Å, and $\beta = 107.70$ (1)° are based on a least-squares refinement of the diffractometer setting angles for 25 reflections with 2θ values between 28° and 30° and with Mo Kα radiation.

Intensities were measured by the ω–2θ scan method. Six standard reflections were measured after every 150 reflections and indicated that the crystal was stable during the course of data collection. Data reduction and all additional calculations were done with the TEXSAN package of crystallographic programs.[24]

The structure was solved by the direct-methods program MITHRIL,[25] where all the non-hydrogen atoms appeared on an electron density map. The choice of enantiomer was made arbitrarily. Many of the hydrogen atoms were located on a difference electron density map after the anisotropic stage of refinement had been reached. All of the hydrogen atoms were subsequently added to the model as fixed contributions at calculated positions with the assumptions C–H = 0.98 Å and $B_H = 1.2B_{eq}$ (attached carbon atom). The methyl hydrogen atoms were idealized to sp^3 geometry based on their locations in the difference electron density map. A secondary extinction coefficient was refined in the final cycles of least squares; a value of 1.7 (1) × 10^{-5} was obtained for this parameter. The final refinement cycle for the 1509 intensities with $F_o^2 > 3\sigma(F_o^2)$ and the 190 variables (anisotropic non-hydrogen atoms and hydrogen atoms fixed) gave agreement indices of $R = 0.040$ and $R_w = 0.047$. The final difference electron density map contained maximum and minimum peak heights of 0.15 and −0.12 e/Å^3. Scattering factors were obtained from the usual sources.[26]

Acknowledgment. We are grateful to the National Institutes of Health for their financial support by means of Grant GM-28468, to George Maynard for valuable assistance with the calculations, and to Susan Reid for her help with the solution and refinement of **30** and **53**.

Supplementary Material Available: Stereodrawings of the unit cells and tables of torsion angles, final positional parameters, and final thermal parameters as well as ORTEP drawings of the four molecules in the asymmetric unit of **35** (22 pages); tables of structure factors for **18**, **30**, and **53** (33 pages). Ordering information is given on any current masthead page.

Comparative Analysis of Molecular-Recognition Levels Attained during Capture of Chiral Cyclopentenyl Organometallics by Conformationally Immobilized Ketonic Systems

Leo A. Paquette,* Wei He, and Robin D. Rogers[1]

Departments of Chemistry, The Ohio State University, Columbus, Ohio 43210, and Northern Illinois University, DeKalb, Illinois 60115

Received February 14, 1989

The diastereoselectivity of the reactions of the chiral organocerates **10**, **15**, **20**, and **22** with β,γ-unsaturated ketones **1** and **7** is described. The reactions involving the tricyclic substrate **7** exhibit excellent π-facial stereoselectivity (syn to the double bond) and are respectably diastereoselective when **10** (11:1) and **15** (8.1:1) are involved. In the case of the bicyclic **6**, there is continued preference for nucleophilic capture syn to the double bond; however, the absence of the cyclopropane ring is accompanied by a dropoff in molecular-recognition capability. Stereochemical assignments were made by NMR correlations and defined unequivocally in four cases by X-ray crystallographic analysis of the anionic oxy-Cope rearrangement products. The stereochemistries of these bridgehead unsaturated ketones reveal in addition that chair-like transition states are adopted during the sigmatropic reorganizations. The results clearly show that the particular substitution pattern in the vinyl organometallic is a significant variable in determining diastereoselectivity. Those interactions considered most important have been analyzed by MODEL calculations. Nonbonded interactions in the interstitial space following complexation of cerium to oxygen and adoption of a somewhat obtuse trajectory give evidence of exerting the greatest control.

Our understanding of the extent and direction of single or double diastereoselection[2] attainable during nucleophilic additions of chiral vinyl organometallics to β,γ-unsaturated ketones is currently founded on a limited number of case studies.[3] These have involved 7,7-disubstituted 5-norbornen-2-ones (1),[4] 7-methyl-7-vinylbicyclo[3.2.0]hept-2-

(1) Author to whom queries regarding the X-ray crystallographic analyses should be directed at the Northern Illinois University address.

(2) (a) Izumi, Y.; Tai, A. *Stereodifferentiating Reactions*; Academic Press: New York, 1977. (b) Masamune, S.; Choy, W.; Petersen, J. S.; Sita, L. R. *Angew. Chem., Int. Ed. Engl.* **1985**, *24*, 1.

(3) Paquette, L. A. In *Organic Synthesis: Modern Trends*; Chizhov, O., Ed.: Blackwell Scientific Publications: Oxford, 1988, pp 1–12.

(4) (a) Paquette, L. A.; Learn, K. S. *J. Am. Chem. Soc.* **1986**, *108*, 7873. (b) Paquette, L. A.; Learn, K. S.; Romine, J. L.; Lin, H.-S. *Ibid.* **1988**, *110*, 879.

0022-3263/89/1954-2291$01.50/0

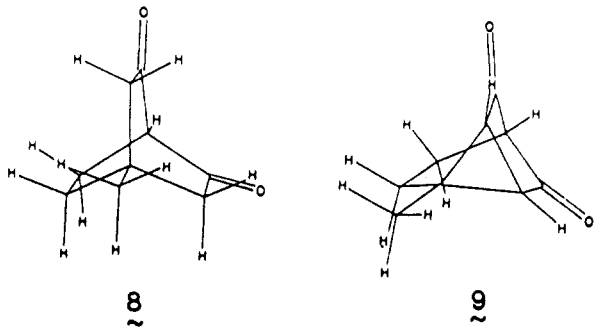

8 9

Figure 1. Ground-state conformations of diketones 8 and 9 as determined by MODEL calculations.

en-6-one (2),[5] (*R*)-(−)-isopiperitinone (3),[6] 3-methoxy-2,7,7-trimethylbicyclo[2.2.2]oct-2-en-5-one (4),[7] and *cis*-8-methylenebicyclo[4.2.0]octan-2-ones such as 5.[8] The resulting alcohols hold considerable potential in stereoselective synthesis since they possess the especially powerful capacity for engaging efficiently in internal chirality transfer via anionic oxy-Cope rearrangement.[9] Through application of this methodology, we have been developing approaches to the ophiobolins,[10] ikarugamycin,[11] forskolin,[7,12] and cerorubenic acid-III[13] that are at once potentially expedient and stereochemically defined.

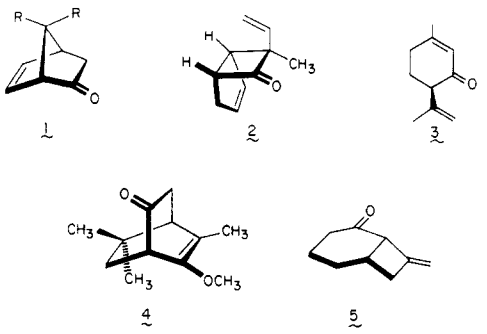

1 2 3 4 5

In continuation of a program designed to probe those discriminatory factors that influence diastereoselection in these carbonyl condensation reactions, we have now investigated the consequences of exposing the pair of racemic bridged ketones 6 and 7[14] to several chiral cyclopentenyl anions. While both systems can be considered to be conformationally rigid, MODEL calculations[15] on diketones

6 7

(5) Paquette, L. A.; Learn, K. S.; Romine, J. L. *Synth. Commun.* **1987**, *17*, 1141; *Tetrahedron* **1987**, *43*, 4989.
(6) Paquette, L. A.; DeRussy, D. T.; Cottrell, C. E. *J. Am. Chem. Soc.* **1988**, *110*, 890.
(7) Paquette, L. A.; Oplinger, J. A. *Tetrahedron* **1989**, *45*, 107.
(8) Paquette, L. A.; DeRussy, D. T.; Gallucci, J. C. *J. Org. Chem.*, preceding paper in this issue.
(9) Hill, R. K. In *Asymmetric Synthesis*; Morrison, J. D., Ed.; Academic Press: New York, 1984; Vol. III, Chapter 8.
(10) (a) Paquette, L. A.; Andrews, D. R.; Springer, J. P. *J. Org. Chem.* **1983**, *48*, 1148. (b) Paquette, L. A.; Colapret, J. A.; Andrews, D. R. *Ibid.* **1985**, *50*, 201.
(11) Paquette, L. A.; Romine, J. L.; Lin, H.-S. *Tetrahedron Lett.* **1987**, *28*, 31.
(12) Oplinger, J. A.; Paquette, L. A. *Tetrahedron Lett.* **1987**, *28*, 5441.
(13) Paquette, L. A.; Poupart, M.-A. *Tetrahedron Lett.* **1988**, *29*, 273.
(14) Poupart, M.-A.; Paquette, L. A. *Tetrahedron Lett.* **1988**, *29*, 269.
(15) (a) Still, W. C.; MacPherson, L. J.; Harada, T.; Rheingold, A. *Tetrahedron* **1984**, *40*, 2275. (b) Still, W. C.; Galynker, I. *Ibid.* **1981**, *37*, 3981.

Table I. Diastereoselectivity Ratios for the Addition of Vinylcerium Reagents to 6 (THF Solution, −78 °C)

organometallic	combined yield, %	endo products (%)	exo products (%)
10	87	**11A** (5), **11B** (1)	**11C** (20), **11D** (61)
		0.25:<0.1	1.0:3.1
15	77	**16A** (5), **16B** (4)	**16C** (20), **16D** (48)
		0.25:0.20	1.0:2.4
20	84	**21A** (12), **21B** (7)	**21C** (25), **21D** (40)
		0.5:0.28	1.0:1.6
22	79	**23A** (6), **23B** (17)	**23C** (15), **23D** (41)
		0.4:1.1	1.0:2.7

Table II. Diagnostic Cyclopentenyl Proton Chemical Shift Data for Adducts to 6 (δ, 300 MHz, C_6D_6 Solution)

	series			
compd	A	B	C	D
11	5.69	5.62	5.43	5.49
16	5.47	5.40	5.34	5.42
21	5.41	5.35	5.28	5.33
33	5.56	5.48	5.55	5.55

8 and 9 (Figure 1) reveal that bridging with an additional (cyclopropane) bond has the consequence of splaying the carbonyl groups in a more outwardly direction. The addition of vinylmagnesium bromide to 8 proceeds, much like in the case of 6-methylenebicyclo[2.2.2]octan-2-one,[16] with a syn/anti stereoselectivity approximating 3.3:1.[17] Closely similar diastereofacial partitioning was anticipated for 6. On the other hand, the ability of 7 to capture nucleophiles syn to its double bond should be considerably enhanced. Indeed, vinylmagnesium bromide has been reported to furnish exclusively the syn adduct (98%) in this case.[13]

In addition to this encouraging prognosis, we considered it highly probable that 7 might enjoy a higher capacity than 6 for exercising diastereomeric recognition in their reactions with chiral nucleophiles. Since the key intermolecular interactions are of steric origin, the additional bond in 7 could affect the more important approach channels. However, it was unknown to what extent the outward splaying discussed above might offset this structural advantage. As a consequence, proper comparative evaluation of the recognition patterns shown by 6 and 7 was anticipated to be informative in relation to the interplay of intermolecular effects central to carbonyl nucleophilic addition reactions.

Results

The 5-Isopropylcyclopentenyl Probe. In order to minimize the wholesale tendency of 6 to enolize when exposed to vinyllithium reagents, recourse has been made throughout this study to the less basic dichlorocerium reagents.[18] When 6 was treated with 10[8] in cold tetrahydrofuran solution, four alcohols were produced. Provided that proper consideration was given to the sensitivity of **11A–D** to certain adsorbents, each could be obtained pure by chromatography in a combined yield of 87%. The two minor products **11A** and **11B** (Table I) were easily recognized to be those diastereomers resulting from anti addition, because their cyclopentenyl olefinic protons in C_6D_6 solution appear 0.1–0.3 ppm to higher field than their counterparts in **11C** and **11D** (Table II). This effect presumably stems from adoption by the latter pair of al-

(16) Martin, S. F.; White, J. B.; Wagner, R. *J. Org. Chem.* **1982**, *47*, 3190.
(17) Poupart, M.-A., unpublished results.
(18) (a) Imamoto, T.; Sugiura, Y.; Takiyama, N. *Tetrahedron Lett.* **1984**, *25*, 4233. (b) Imamoto, T.; Sugiura, Y. *J. Organomet. Chem.* **1985**, *285*, C21. (c) Imamoto, T.; Takiyama, N.; Nakamura, K. *Tetrahedron Lett.* **1985**, *26*, 4763.

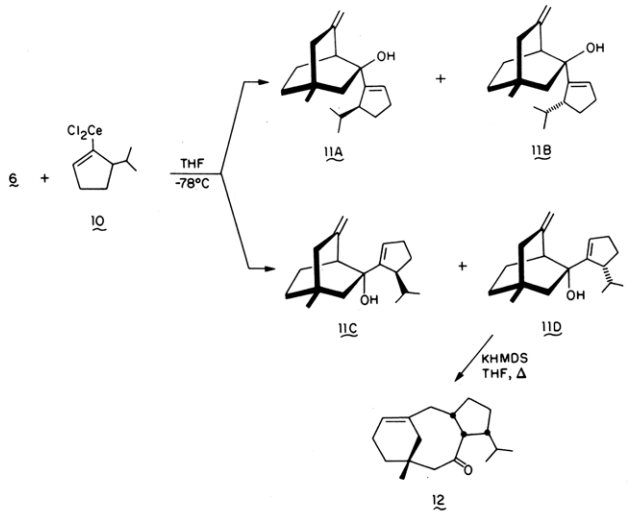

cohols of a conformation where diamagnetic shielding by the exocyclic double bond can operate at the terminus of the allylic alcohol moiety.[16]

That the relative configurational assignments shown in **11C** and **11D** are indeed correct was established by anionic oxy-Cope rearrangement of **11D** and X-ray analysis of the nicely crystalline ketone **12** (Table III, Figure 2). For proximity reasons, **11A** and **11B** were not expected to undergo similar [3,3] sigmatropy, and they do not. However, **11C** likewise failed to isomerize when heated in tetrahydrofuran solution with potassium hexamethyldisilazide despite the *apparent* proper stereodisposition of its diene double bonds. While a suitable chair alignment of the unsaturated centers can be realized in **11D** (see M), attainment of a similar internal geometry in **11C** is precluded by the close proximity of the isopropyl side chain to the alkoxide center (as in N).

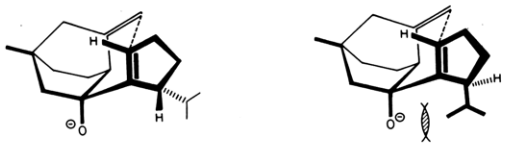

The diastereoselective discrimination observed during the condensation of **6** with **10** favored **11D** over **11C** by a factor of 3.1:1. Substitution of **7** for **6** in this reaction, with care to reproduce reaction conditions as closely as possible, gave rise to a two-component product mixture consisting chiefly of **13B** (Table IV). Neither possible

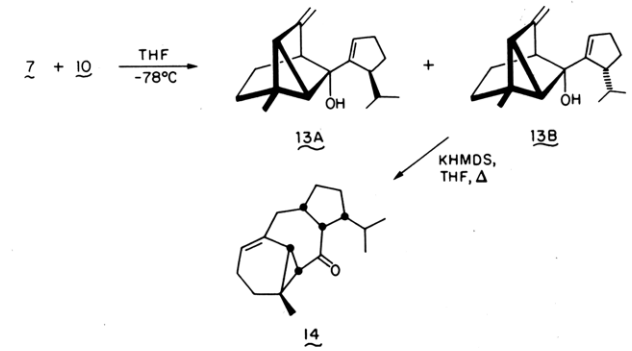

alcohol resulting from anti addition was found. Although pure **13A** and **13B** are easily distinguished by ^{1}H NMR spectroscopy in C_6D_6 solution (Table IV), the stereodisposition of the isopropyl group could not be unequivocally ascertained on this basis alone. Consequently, **13B** was isomerized to **14** and recourse was again made to crystallographic analysis (Figure 3).

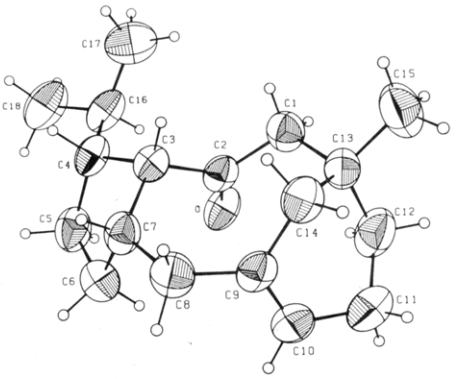

Figure 2. Computer-generated perspective drawing of **12** as determined by X-ray crystallography. The atom numbering is arbitrary.

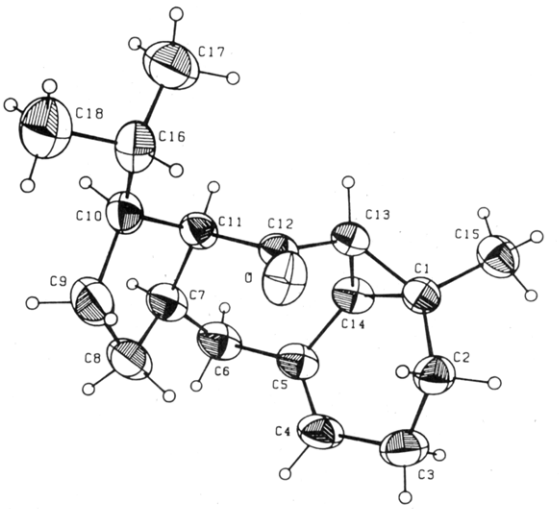

Figure 3. Computer-generated perspective drawing of **14** as determined by X-ray crystallography. The atom numbering is arbitrary.

Having thus ascertained that **13B** predominates by a wide margin, we see that both **6** and **7** respond to **10** more favorably when passing through those syn transition states that give rise to the respective α-isopropyl alcohols. The effectiveness of **7** in achieving this discrimination is more than 3 times greater than that of **6**. Added insight into the principal differences between these bonding pathways was gained by analyzing the case studies that follow.

Consequences of *trans*-4,5-Dialkyl Substitution of the Cyclopentene Nucleophile. The effect of nucleophile structure on product distribution was next extended to encompass **15**,[6] a relevant feature of which is the transoid disposition of its ethyl and methyl groups at C5 and C4, respectively. More specifically, we sought to learn if reduction in the size of the 5-substituent from isopropyl to ethyl could be effectively counteracted by the adjacent antiplanar methyl appendage. As expected, the four alcohols **16A–D** were generated during this condensation (Table I). Usefully, these diastereomers proved amenable to chromatographic separation (77% combined isolated yield). Once again, the pair of minor products were considered to arise from exterior attack. Analysis of their ^{1}H NMR spectra called attention to the fact that the cyclopentenyl olefinic proton in **16A** appears downfield of that in **16B** (Table II). Consistency demanded that the indicated relative stereochemistries be adopted.

Configurational assignments to **16C** and **16D** were likewise initially based on the fact that the cyclopentenyl proton in **16D** is more deshielded than that in **16C** (Table

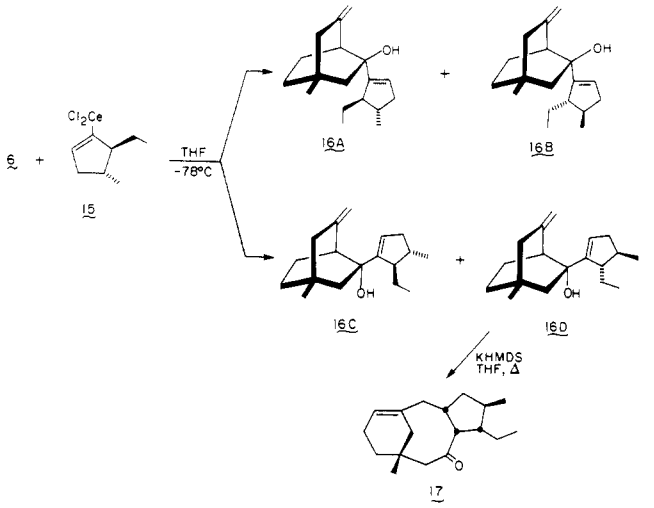

II). Extrapolation of the spectroscopic features of alcohols **11** to those of **16** was considered advisable for at least two reasons: (a) the substitution plans in the cyclopentenyl sectors of these molecules were not considered to be sufficiently different to exert major ground state conformational changes; (b) in the absence of major structural perturbations, the anisotropic contributions of the hydroxyl group and π bonds as well as those from the solvent should impact chemical shifts in closely comparable ways. The validity of these conclusions was subsequently established by anionic oxy-Cope rearrangement of **16C** to **17** and by three-dimensional crystal structure analysis of this ketone (Table III, Figure 4). Once again, the ability to construct rapidly a functionalized tricyclic bridgehead alkene having several stereogenic centers had been demonstrated. The relative configurations of the five asymmetric carbon atoms in **17** necessitate that **16D** be its progenitor.

The conversion of **7** to **18A** and **18B** upon exposure to **15** in tetrahydrofuran at −78 °C proceeded quite efficiently (91%). In this case, the kinetic fractionation was seen to

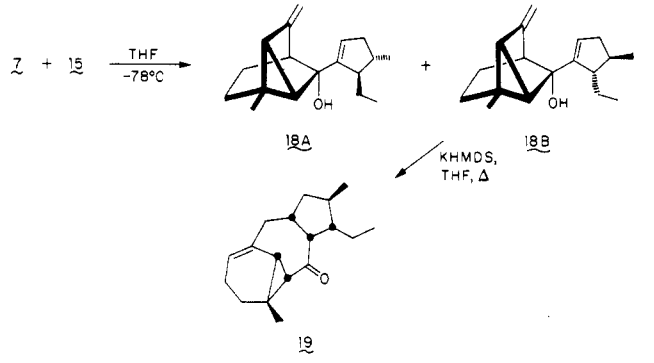

drop to 8:1. The assignment of relative stereochemistry to these readily separated reaction products was based on comparison of their 300-MHz ^{1}H NMR spectra in C_6D_6, the cyclopentenyl proton in **18B** being the more shielded. When **18B** was heated with potassium hexamethyldisilazide in tetrahydrofuran, isomerization to **19** was realized (85%).

The combined data demonstrate that the capacity of **15** for double diastereoselection during condensation with **6** and **7** is somewhat lower than that exhibited by **10**, but still quite respectable. Would cis-4,5-disubstitution of the nucleophile result in improved stereochemical discrimination? To answer this question, the consequences of condensing **6** and **7** with dichlorocerates **20** and **22** were examined as described below.

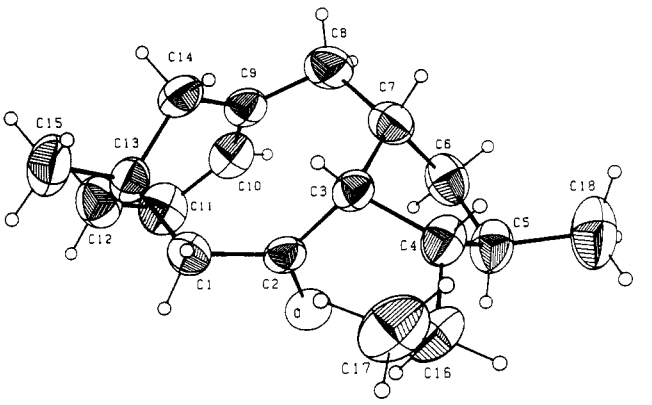

Figure 4. Computer-generated perspective drawing of **17** as determined by X-ray crystallography. The atom numbering is arbitrary.

Kinetic Fractionations Associated with Cis-Bicyclic Cerates. The response of **6** to **20**[6] followed the general pattern of giving rise to four adducts (**21A–D**), which were chromatographically separated and characterized. The ^{1}H NMR data compiled in Table II provide

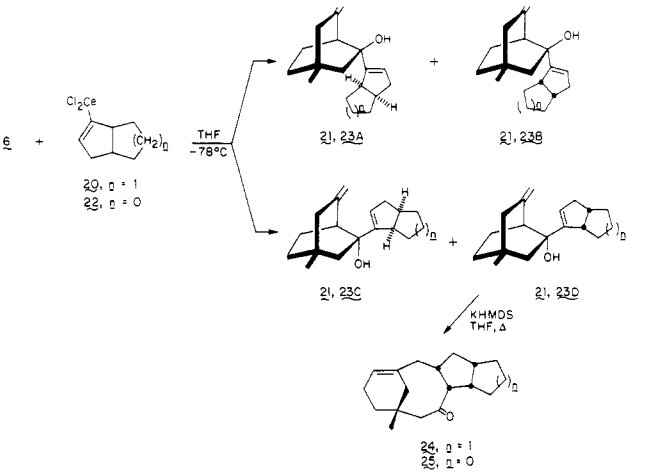

evidence that these alcohols can easily be assigned to one series or the other. [3,3] sigmatropy within major product **21D** provided the opportunity to transfer its relative stereochemistry intramolecularly into that found in ketone **24**. Quite strikingly, the ratio of **D**:**C** diastereomers had now dropped to the lowest value encountered so far (1.6). Clearly, the structural features present in **20** are the least conducive for utilitarian intermolecular discrimination during the condensation process.

The same pattern was to unfold following the condensation of **20** with **7**. In this instance, two alcohols were formed with 1:2.2 diastereoselectivity. For unknown reasons, major product **26B** does not exhibit its cyclopentenyl proton downfield of that displayed by **26A** (Table IV).

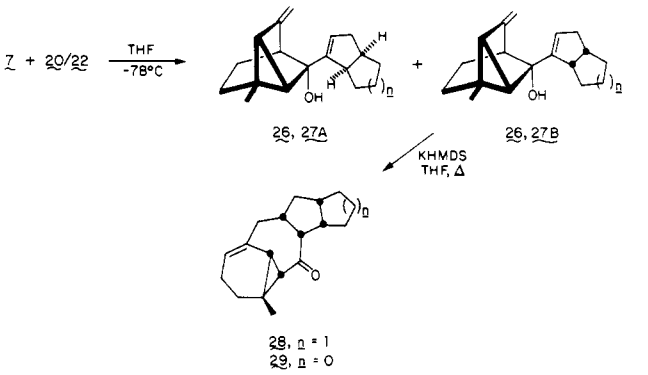

Table III. Crystal Data and Summary of Intensity Data Collection and Structural Refinement for 12, 14, and 17

	12	14	17
color/shape	colorless/parallelepiped	colorless/fragment	colorless/parallelepiped
fw, amu	260.4	258.4	260.42
space group	$P2_1/n$	$P2_1/c$	$P2_1/c$
temp, °C	20	20	20
cell constants[a,d,e]			
a, Å	8.322 (3)	20.065 (7)	15.314 (4)
b, Å	20.615 (7)	7.587 (4)	9.583 (1)
c, Å	9.211 (5)	9.806 (3)	11.013 (5)
β, deg	102.22 (4)	91.82 (2)	103.88 (3)
cell vol, Å^3	1544	1492	1569
formula units/unit cell	4	4	4
D_{calcd}, g cm^{-3}	1.12	1.15	1.10
μ_{calcd}, cm^{-1}	0.35	0.36	0.34
diffractometer/scan	Enraf-Nonius CAD-4/θ–2θ	Enraf-Nonius CAD-4/θ–2θ	Enraf-Nonius CAD-4/θ–2θ
radiatn, graphite monochromator	Mo Kα (λ = 0.71073)	Mo Kα (λ = 0.71073)	Mo Kα (λ = 0.71073)
max cryst dimens, mm	0.13 × 0.30 × 0.45	0.35 × 0.43 × 0.55	0.40 × 0.40 × 0.50
scan width	0.80 + 0.35(tan θ)	0.80 + 0.35(tan θ)	0.80 + 0.35(tan θ)
standard reflctns	400; 0,10,0; 008	13,0,0; 040; 006	12,0,0; 060, 004
decay of stds, %	−1.1	±2	±3
reflctns measd	2767	2967	3069
2θ range, deg	2 ≤ 2θ ≤ 50	2 ≤ 2θ ≤ 50	2 ≤ 2θ ≤ 50
range of h,k,l	+9,+24,±10	±18,+11,+13	±18,+11,+13
reflctns obsd [$F_o \geq 5\sigma(F_o)$][b]	1400	1934	1580
computer programs	SHELX[25]	SHELX[25]	SHELX[25]
structure soln	MULTAN[27]	MULTAN[27]	MULTAN[27]
no. of parameters varied	172	172	172
weights	$[\sigma(F_o)^2 + 0.00008F_o^2]^{-1}$	$[\sigma(F_o)^2 + 0.00003F_o^2]^{-1}$	$[\sigma(F_o)^2 + 0.0004F_o^2]^{-1}$
GOF	0.91	2.21	1.1
$R = \Sigma\|\|F_o\| - \|F_c\|\|/\Sigma\|F_o\|$	0.053	0.054	0.051
R_w	0.055	0.057	0.060
largest feature in final diff map	0.2 e Å^{-3}	0.3 e Å^{-3}	0.2 e Å^{-3}

[a] Least-squares refinement of $((\sin\theta)/\lambda)^2$ values for 21 reflections $\theta > 20°$ for 12. [b] Corrections: Lorentz polarization. [c] Neutral scattering factors and anomalous dispersion corrections from ref 26. [d] Least-squares refinement of $((\sin\theta)/\lambda)^2$ values for 25 reflections $\theta > 18°$ for 14. [e] Least-squares refinement of $((\sin\theta)/\lambda)^2$ values for 25 reflections $\theta > 20°$ for 17.

Table IV. Diastereoselectivity Ratios (THF, −78 °C) and Diagnostic Cyclopentenyl Proton Chemical Shift Data (δ, 300 MHz, C_6D_6) for Adducts to 7

organometallic	combined yield, %	A series (% isolated)	δ	B series (% isolated)	δ
16	85	**13** (7)	5.75	**13** (78)	5.56
			1.0:11.0		
17	91	**18** (10)	5.48	**18** (81)	5.42
			1.0:8.1		
20	70	**26** (22)	5.63	**26** (48)	5.68
			1.0:2.2		
22	78	**27** (24)	5.52	**27** (53)	5.45
			1.0:2.2		

However, the remainder of its spectral characteristics conform fully to expectations for the assigned structure. These include the deshielded nature of its allylic bridgehead (δ 3.46) and the exocyclic methylene protons (δ 4.78, 4.67) relative to those encountered in **26A** (δ 3.38; 4.75, 4.63), as well as the typically more shielded position of its tertiary allylic cyclopentenyl proton (δ 2.27) when compared to that of **26A** (2.30). The Experimental Section is replete with analogous diagnostic chemical-shift comparisons.

We see therefore that **20** emerges as a reagent having the minimum degree of impact on the stereocontrolled elaboration of the carbinol center. Once **26B** has been separated, however, its oxy-Cope rearrangement to **28** provides for the convenient construction of a pentacyclic ketone having seven stereogenic carbon atoms.

Since simple permutation of the nucleophile structure from bicyclo[3.3.0]octenyl to bicyclo[3.2.0]heptenyl has in an earlier study[4] resulted in notable modification of stereoselection, the last phase of this investigation involved condensation of **22**[6] with **6** and **7**. Interestingly, whereas the **27B**:**27A** ratio (2.2) proved to be identical with that realized for **20** (Table IV), the relative proportion of

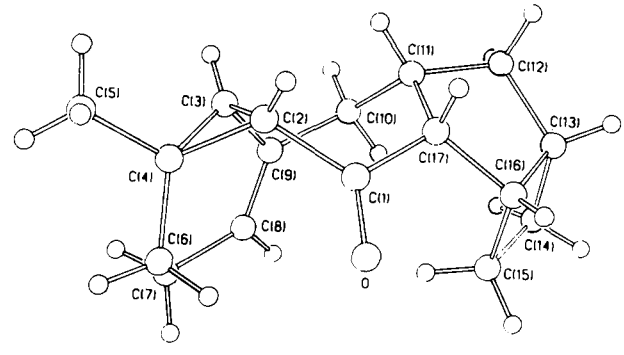

Figure 5. Computer-generated perspective drawing of **29** as determined by X-ray crystallography (courtesy of A. L. Rheingold, University of Delaware).

23D:**23C** increased to 2.5:1. This level of diastereoselection is larger than that encountered with both **15** and **20** and actually approaches the partitioning factor seen for **10** (Table I). Accordingly, small structural differences within the organocerate can impact sensitively on the capacity of **6** and **7** to attain useful levels of molecular recognition.

As before, **23D** was isomerized to **25**, and **27B** was transformed into ketone **29**. Unequivocal characterization of the latter end product was achieved by X-ray crystallography (Figure 5) in order to reconfirm the merits of the structural systemization improvised on the basis of ^{1}H NMR analysis.

Discussion

Transition-State Model for the Carbonyl Addition Step. For ketones **6** and **7**, coupling to the various organocerates proceeds under kinetic control via sets of diastereomeric pathways. Consequently, the ratios of products are determined entirely by the relative energies of the

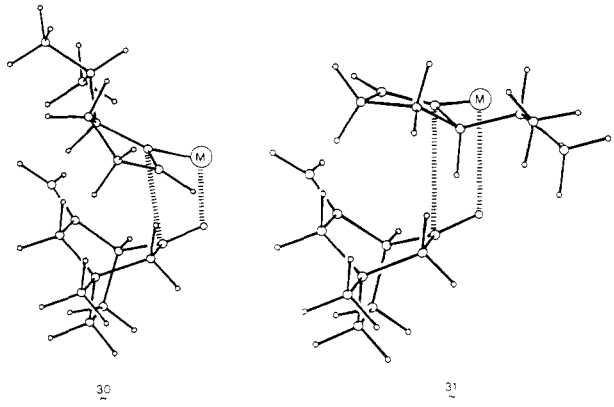

Figure 6. Diastereomeric transition state models for the addition of **10** to **6**. Arrangement **31** leads to **11D** and is favored. The intermolecular distance has been arbitrarily selected.

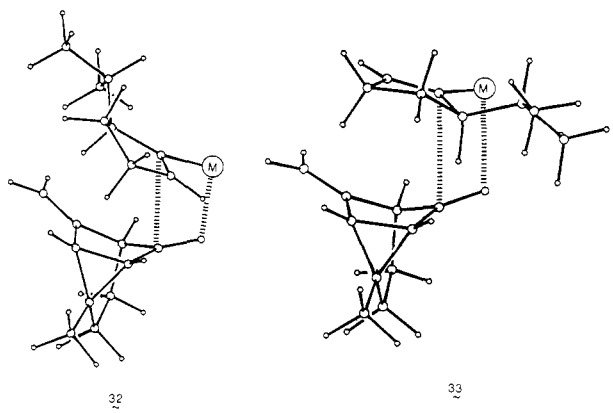

Figure 7. Diastereomeric transition state models for the addition of **10** to **7**. Arrangement **33** leads to **13B** and is favored. The intermolecular distance has been arbitrarily selected.

various transition-state structures associated with the rate-determining steps.[19] Our selection of the appropriate transition structures is founded upon application of the Bürgi–Dunitz model for the directionality of nucleophilic capture by the carbonyl group[20] following complexation of the cerium to oxygen.[4,8,21] Analysis of carbanion attack on a carbonyl carbon has not been accomplished computationally since such processes have no apparent activation energy in the gas phase.[22] Nevertheless, a somewhat obtuse trajectory of attack can logically be assumed to operate since it maximizes interaction of the nucleophile HOMO with the carbonyl LUMO.[23]

As the highest energy point along the lowest energy transit from reactants to product is approached, the ketone and organometallic can be expected to select a variety of geometries. In order to obtain qualitative estimates of the relevant energetic costs of the various reasonable combinations, we have performed MODEL calculations[15] on each of the ketones and vinyl cerates in order to realize their lowest energy conformations. Following acquisition of this information, the various combinations were examined qualitatively with an aim to minimize *intermolecular* steric interactions to the maximum extent. Of course, any structural distortion that might materialize within the activated complex cannot be addressed under these circumstances. Notwithstanding, the predictive power of the method is very good. The preferred matched diastereomer relationship was arrived at in every instance. Estimates of the energetic imbalances between the diastereomeric transition states were not attempted, nor should they be.

As suggested in the introduction, the geometries of **6** and **7** differ appreciably. As **10** begins to position itself into that arrangement most ideal for bonding to either of these substrates, the effects of nonbonding steric interaction become paramount. Those trajectories of attack involving orientation of the isopropyl group in **10** toward the bicyclic framework of either ketone are obviously disfavored strongly. When the alternative cyclopentenyl surface is utilized as shown in Figures 6 and 7, there is seen in **31** and **33** more optimal staggering of the interstitial C–H bonds relative to those scenarios present within **30** and **32**. However, the distinction between **30** and **31** is not as striking as the distinction between **32** and **33**. A major consequence of the interconnective cyclopropane bond is pronounced outward splaying of the protons attached to the three-membered ring. In the models, this pair of C–H bonds is very much projected external to the tricyclic framework, with the result that a greater steric disparity materializes in the upper-left and upper-right rear octants of the carbonyl group as drawn. This feature also plausibly explains the heightened diastereoselective abilities of **7** relative to **6**, where steric factors in these sectors are more closely balanced.

The improved discriminatory capacity of **10** relative to **15**, **20**, and **22** seemingly originates from the heightened puckering of the five-membered ring in this nucleophilic species when compared to the others. Its isopropyl substituent seeks to gain equatorial status and, in so doing, induces the generation of a relatively robust envelope conformation. In **15**, the trans-oriented methyl and ethyl groups do not reinforce each other in shaping a well-defined envelope geometry because of the onset of eclipsing interactions. Moreover, the spatial disposition of the substituents is not especially conducive to the lowering of interstitial steric congestion. The situation is further exacerbated by ring fusion in **20** and **22**. Puckering within the cyclopentene ring is severely impeded under these circumstances. Nevertheless, the relative energies of different diastereomeric approaches to **7** remain sufficiently disparate to make matters synthetically attractive.

Stereochemical Options Associated with the Oxy-Cope Process. In view of the number of stereogenic centers present in the several alcohol condensation products, we sought to take advantage of efficient chirality transfer normally attainable by means of [3,3] sigmatropy.[9] As a consequence of the intramolecularity of the oxyanionic Cope process, the various stereochemical elements intrinsic to these alcohols are not independent variables. One option does remain, however, and this has to do with whether the rearrangement transition state develops chair-like or boat-like characteristics. Highly ordered structural features are demanded of either activated complex, the consequences being that knowledge of product stereochemistry often serves to clarify the precise course of events. This is true here.

(19) (a) DeTar, D. F. *J. Org. Chem.* **1986**, *51*, 3749. (b) Zefirov, N. S. *Tetrahedron* **1977**, *33*, 2719.

(20) (a) Bürgi, H. B.; Dunitz, J. D.; Shefter, E. *J. Am. Chem. Soc.* **1973**, *95*, 5065. (b) Bürgi, H. B.; Dunitz, J. D. *Acc. Chem. Res.* **1983**, *16*, 153 and pertinent references cited therein.

(21) (a) Houk, K. N.; Rondan, N. G.; Schleyer, P. von R.; Kaufmann, E.; Clark, T. *J. Am. Chem. Soc.* **1985**, *107*, 2821. (b) Kaufmann, E.; Schleyer, P. von R.; Houk, K. N.; Wu, Y.-D. *Ibid.* **1985**, *107*, 5560.

(22) (a) Bürgi, H. B.; Dunitz, J. D.; Lehn, J. M.; Wipff, G. *Tetrahedron* **1974**, *30*, 1563. (b) Scheiner, S.; Lipscomb, W. N.; Kleier, D. A. *J. Am. Chem. Soc.* **1976**, *98*, 4770. (c) The transition structure for BH_4^- attack on formaldehyde is a recent exception: Eisenstein, O.; Schlegel, H. B.; Kayser, M. M. *J. Org. Chem.* **1982**, *47*, 2886. The H–CO angle is 115°, and the transition structure is very near products.

(23) (a) Klopman, G. In *Chemical Reactivity and Reaction Paths*; Klopman, G., Ed.; Wiley-Interscience: New York, 1974; Chapter 4, pp 55–166. (b) Paddon-Row, M. N.; Rondan, N. G.; Houk, K. N. *J. Am. Chem. Soc.* **1982**, *104*, 7162.

Structures M and P represent the two possible transition states available to the protypical substrate **11D**. Whereas the orientation of the cyclopentenyl double bond in M is such that chair-like characteristics are guaranteed to develop as electronic reorganization begins, the reverse relative positioning of the cyclopentenyl double bond as in P sets the stage for boat-like structural features to materialize. The differing consequences of these incipient

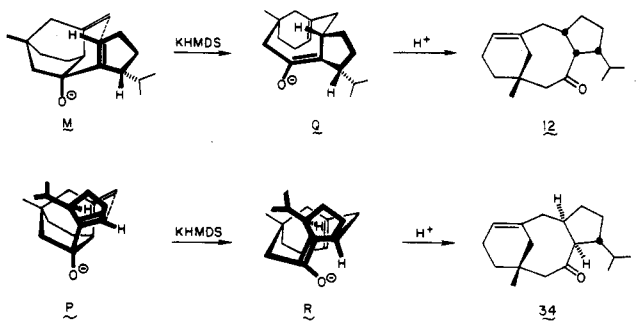

bond-forming schemes are depicted in Q and R. Ensuing protonation of these enolate anions should proceed from the convex surface of the eight-membered ring if kinetically controlled and result in generation of a cis ring juncture in either case. At this point, a distinction is made clearly apparent since in **12** the hydrogens located at the bond common to the five- and eight-membered rings are oriented syn to the transannularly positioned methylene bridge, while in **34** they are anti.

These first principles of conformation theory, when combined with the exclusive isolation of **12** at the experimental level, reveal unequivocally that the chair alternative is most energetically accessible to **11D**. The crystallographic data obtained for **14**, **17**, and **29** confirm that **13B**, **16D**, and **27B** behave in entirely similar fashion. Thus, conventional concertedness is most readily accommodated in these systems within chair-like arrangements of type M, irrespective of whether a cyclopropane ring is present or not. We attribute this unidirectionality to the added energy costs generally associated with boat-like geometries.[9,24] To the extent that this reaction channel can be relied upon to operate, the two-step process outlined here is seen to enable rapid construction of relatively complex polycyclic molecules having multiple chiral centers.

Experimental Section

Prototypical Organocerium Addition to 6 and 7. Cerium trichloride heptahydrate (490 mg, 1.3 mmol) was heated at 140–150 °C for 2.5 h at 0.1 Torr and allowed to cool. Anhydrous tetrahydrofuran (8 mL) was introduced, and the suspension was stirred magnetically for 3 h under nitrogen. In a separate flask, 1-bromo-5-isopropylcyclopentene[6] (227 mg, 1.2 mmol) in 8 mL of dry tetrahydrofuran was cooled to −78 °C, and *tert*-butyllithium (1.4 mL of 1.7 M, 2.4 mmol) was added dropwise. The cold yellow solution was stirred for 30 min and transferred via cannula to the now cold (−78 °C) cerium chloride slurry. The resulting orange-colored mixture was stirred at −78 °C for 1 h, at which point a solution of **6**[14] (150 mg, 1.0 mmol) in 1.5 mL of dry tetrahydrofuran was added dropwise. The reaction mixture was stirred at this temperature for 2.5 h, quenched at −78 °C with 2 mL of saturated ammonium chloride solution, and diluted with brine (5 mL). The products were extracted into ether (3 × 10 mL), and the combined organic phases were washed with 10% hydrochloric acid (10 mL), saturated sodium bicarbonate solution (10 mL), and brine (10 mL) prior to drying and solvent evaporation. The composition of the yellow oily residue was quantified by analytical HPLC (SiO_2, elution with 2% ethyl acetate in hexane), and the individual components were separated on a preparative scale by MPLC (SiO_2, elution with 4% ether in petroleum ether): 12 mg (5%) of **11A**, 53 mg (20%) of **11C**, 4 mg (1%) of **11B**, and 158 mg (61%) of **11D** (combined yield = 87%).

For **11A**: colorless oil; IR (neat, cm^{-1}) 2940, 2860, 1460, 1450, 1380, 1370, 1360, 1060, 880; ^1H NMR (300 MHz, C_6D_6) δ 5.69 (s, 1 H), 4.88 (m, 1 H), 4.79 (m, 1 H), 2.77 (m, 1 H), 2.65 (m, 1 H), 2.35 (t, J = 3.0 Hz, 1 H), 2.20 (m, 2 H), 2.07 (dd, J = 2.7, 14 Hz, 1 H), 1.93 (dd, J = 2.2, 13 Hz, 1 H), 1.82 (m, 2 H), 1.75 (s, 1 H), 1.52 (m, 2 H), 1.37 (d, J = 14 Hz, 2 H), 1.07 (m, 2 H), 1.01 (d, J = 6.8 Hz, 3 H), 0.95 (d, J = 6.8 Hz, 3 H), 0.75 (s, 3 H); ^{13}C NMR (75 MHz, C_6D_6) (ppm) 149.65, 148.31, 128.65, 110.42, 73.21, 51.81, 50.13, 46.35, 41.36, 32.12, 31.64, 31.31, 30.60, 27.43, 24.73, 22.99, 22.52, 16.14; MS m/z (M^+) calcd 260.2140, obsd 260.2135.

For **11B**: colorless liquid: ^1H NMR (300 MHz, C_6D_6) δ 5.62 (m, 1 H), 4.84 (m, 1 H), 4.71 (m, 1 H), 2.94 (m, 1 H), 2.47 (m, 1 H), 2.43–2.30 (m, 2 H), 2.23–2.11 (m, 2 H), 1.96 (dd, J = 13.8, 2.9 Hz, 1 H), 1.89 (m, 1 H), 1.77 (m, 2 H), 1.64–1.07 (series of m, 4 H), 0.98 (d, J = 6.9 Hz, 3 H), 0.87 (m, 2 H), 0.79 (d, J = 6.7 Hz, 3 H), 0.78 (s, 3 H); MS m/z (M^+) calcd 260.1240, obsd 260.2154.

For **11C**: colorless liquid; IR (neat, cm^{-1}) 3500, 2940, 2860, 1460, 1450, 1380, 1360, 890, 880; ^1H NMR (300 MHz, C_6D_6) δ 5.43 (m, 1 H), 4.89 (m, 1 H), 4.82 (m, 1 H), 3.13 (m, 1 H), 2.40 (m, 1 H), 2.36 (t, J = 3.0 Hz, 1 H), 2.23 (m, 2 H), 2.07 (dd, J = 2.4, 17 Hz, 1 H), 1.90 (dd, J = 2.4, 17 Hz, 1 H), 1.80 (m, 2 H), 1.77 (m, 2 H), 1.67 (s, 1 H), 1.53 (dd, J = 2.4, 14 Hz, 2 H), 1.09 (m, 2 H), 1.00 (d, J = 6.9 Hz, 3 H), 0.82 (d, J = 6.9 Hz, 3 H), 0.75 (s, 3 H); ^{13}C NMR (75 MHz, C_6D_6) (ppm) 150.07, 148.67, 126.82, 110.02, 73.16, 51.90, 50.50, 47.46, 41.00, 32.63, 32.43, 31.28, 30.22, 27.45, 23.79, 23.35, 22.60, 15.88; MS m/z (M^+) calcd 260.2140, obsd 260.2151.

For **11D**: colorless liquid; IR (neat, cm^{-1}) 3470, 2940, 2860, 1645, 1460, 1450, 1380, 1360, 1035, 1020, 1010, 980; ^1H NMR (300 MHz, C_6D_6) δ 5.48 (m, 1 H), 4.83 (m, 1 H), 4.76 (m, 1 H), 2.88 (m, 1 H), 2.37 (m, 1 H), 2.27 (m, 1 H), 2.22 (m, 2 H), 1.97 (m, 1 H), 1.80 (m, 1 H), 1.73 (m, 1 H), 1.69 (m, 1 H), 1.47 (m, 2 H), 1.40 (m, 1 H), 1.23 (m, 2 H), 0.96 (d, J = 6.9 Hz, 3 H), 0.84 (m, 2 H), 0.79 (d, J = 6.7 Hz, 3 H), 0.77 (s, 3 H); ^{13}C NMR (75 MHz, C_6D_6) (ppm) 151.10, 149.43, 127.20, 108.59, 73.66, 51.88, 50.57, 47.35, 41.48, 32.66, 31.73, 31.37, 30.10, 27.64, 23.76, 22.62, 22.55, 15.82; MS m/z (M^+) calcd 260.2140, obsd 260.2160.

Anal. Calcd for $C_{18}H_{28}O$: C, 83.01; H, 10.84. Found: C, 82.76; H, 10.91.

Addition of 10 to 7. Reaction of **10** with 150 mg (1.0 mmol) of **7**[14] furnished after MPLC 17 mg (7%) of **13A** and 202 mg (78%) of **13B**.

For **13A**: colorless oil; IR (neat, cm^{-1}) 3540, 3480, 2950, 2875, 1450, 1375, 1065, 1020, 990, 885; ^1H NMR (300 MHz, C_6D_6) δ 5.74 (m, 1 H), 4.76 (d, J = 1.1 Hz, 1 H), 4.68 (s, 1 H), 2.87 (m, 1 H), 2.45 (m, 1 H), 2.32 (s, 1 H), 2.19 (m, 3 H), 1.76 (m, 4 H), 1.65 (d, J = 5.7 Hz, 1 H), 1.60 (d, J = 6.5 Hz, 1 H), 1.55 (m, 1 H), 1.08 (s, 1 H), 0.99 (d, J = 6.9 Hz, 3 H), 0.86 (d, J = 6.8 Hz, 3 H), 0.84 (s, 3 H); ^{13}C NMR (75 MHz, C_6D_6) (ppm) 153.35, 148.49, 126.39, 100.05, 77.29, 50.76, 46.20, 38.77, 34.49, 31.12, 29.10, 27.01, 24.48, 23.51, 23.11, 22.94, 21.47, 15.10; MS m/z (M^+) calcd 258.1984, obsd 258.2025.

For **13B**: colorless oil; IR (neat, cm^{-1}) 3470, 2950, 2900, 2860, 1655, 1460, 1380, 1365, 1085, 1055, 1025, 960, 860; ^1H NMR (300 MHz, C_6D_6) δ 5.56 (m, 1 H), 4.79 (d, J = 1.3 Hz, 1 H), 4.69 (d, J = 0.7 Hz, 1 H), 3.00 (m, 1 H), 2.30 (t, J = 3.0 Hz, 1 H), 2.22 (m, 4 H), 1.76 (m, 4 H), 1.61 (d, J = 5.7 Hz, 1 H), 1.54 (m, 1 H), 1.49 (d, J = 5.7 Hz, 1 H), 1.17 (s, 1 H), 0.98 (d, J = 6.8 Hz, 3 H), 0.83 (s, 3 H), 0.79 (d, J = 6.8 Hz, 3 H); ^{13}C NMR (75 MHz, C_6D_6) (ppm) 153.90, 149.49, 126.80, 101.41, 78.53, 51.56, 47.79, 39.86, 36.08, 32.63, 30.05, 27.59, 25.18, 24.40, 23.93, 23.84, 22.50, 15.65; MS m/z (M^+) calcd 258.1984, obsd 258.1978.

Anal. Calcd for $C_{18}H_{26}O$: C, 83.66; H, 10.15. Found: C, 83.72; H, 10.21.

Addition of 15 to 6. In this instance, the following four alcohols were isolated: **16A** (13 mg, 5%), **16C** (51 mg, 20%), **16B** (9 mg, 4%), **16D** (124 mg, 48%).

(24) Doering, W. v. E.; Roth, W. R. *Tetrahedron* **1962**, *18*, 67.
(25) Sheldrick, G. M. SHELX, a system of computer programs for X-ray structure determination as locally modified (1976).
(26) *International Tables for X-ray Crsytallography*; Kynoch Press: Birmingham, England, 1974; Vol. IV, pp 72, 99, 149.
(27) Germain, G.; Main, P.; Woolfson, M. M. *Acta Crystallogr.* **1971**, *A27*, 368.

For **16A**: colorless liquid; IR (neat, cm^{-1}) 2940, 2920, 2860, 1450, 1370, 1060, 1015, 900, 885; ^1H NMR (300 MHz, C_6D_6) δ 5.47 (m, 1 H), 4.88 (m, 1 H), 4.80 (m, 1 H), 2.59 (ddt, J = 2.0, 7.3, 16.6 Hz, 1 H), 2.28 (m, 1 H), 2.23 (m, 1 H), 2.13 (m, 1 H), 2.02 (dd, J = 2.6, 14.2 Hz, 1 H), 1.88 (dm, J = 16.6 Hz, 1 H), 1.87 (m, 1 H), 1.73 (dm, J = 16.6 Hz, 1 H), 1.60 (m, 2 H), 1.45 (m, 1 H), 1.38 (m, 1 H), 1.07 (m, 2 H), 1.01 (d, J = 7.4 Hz, 3 H), 0.97 (d, J = 17.0 Hz, 3 H), 0.85 (m, 2 H), 0.74 (s, 3 H); ^{13}C NMR (75 MHz, C_6D_6) (ppm) 149.63, 148.25, 125.62, 110.47, 73.22, 55.61, 49.97, 46.22, 41.25, 39.23, 37.45, 31.68, 31.36, 27.41, 27.31, 23.10, 22.69, 12.05; MS m/z (M^+) calcd 260.2140, obsd 260.2144.

For **16B**: colorless liquid; IR (neat, cm^{-1}) 2940, 2910, 2860, 1640, 1450, 1370, 1010, 880; ^1H NMR (300 MHz, C_6D_6) δ 5.40 (m, 1 H), 4.81 (m, 1 H), 4.70 (m, 1 H), 2.49 (ddt, J = 2.1, 7.5, 16.5 Hz, 1 H), 2.37 (t, J = 3.0 Hz, 1 H), 2.31 (m, 1 H), 2.07–1.83 (m, 3 H), 1.93 (dd, J = 3.0, 13.8 Hz, 1 H), 1.86 (dd, J = 2.4, 7.4 Hz, 1 H), 1.72 (dm, J = 16.6 Hz, 1 H), 1.59–1.20 (m, 4 H), 1.31 (dd, J = 2.7, 14.0 Hz, 1 H), 1.18–0.83 (m, 2 H), 0.98 (d, J = 7.0 Hz, 3 H), 0.94 (t, J = 7.3 Hz, 3 H), 0.77 (s, 3 H); MS m/z (M^+) calcd 260.2140, obsd 260.2155.

For **16C**: colorless liquid; IR (neat, cm^{-1}) 2940, 2920, 2860, 1450, 880; ^1H NMR (300 MHz, C_6D_6) δ 5.34 (s, 1 H), 4.90 (m, 1 H), 4.83 (m, 1 H), 2.55 (m, 2 H), 2.37 (m, 1 H), 2.14–1.71 (series of m, 6 H), 1.60–1.37 (m, 4 H), 1.12 (m, 3 H), 1.03 (d, J = 7.0 Hz, 3 H), 0.96 (t, J = 7.3 Hz, 3 H), 0.77 (s, 3 H); ^{13}C NMR (63 MHz, C_6D_6) (ppm) 148.89, 148.73, 124.32, 109.82, 73.01, 55.48, 49.90, 47.51, 40.99, 39.82, 36.74, 32.38, 31.24, 27.41, 27.13, 23.49, 23.13, 11.86; MS m/z (M^+) calcd 260.2140, obsd 260.2152.

For **16D**: colorless oil; IR (neat, cm^{-1}) 3460, 2940, 2910, 2860, 1450, 1015, 970, 875; ^1H NMR (300 MHz, C_6D_6) δ 5.42 (s, 1 H), 4.80 (m, 1 H), 4.75 (m, 1 H), 2.51 (ddt, J = 2.2, 7.8, 16.5 Hz, 1 H), 2.39 (m, 1 H), 2.32 (m, 2 H), 1.95 (m, 2 H), 1.88 (m, 2 H), 1.80 (dt, J = 2.6, 17.0 Hz, 1 H), 1.73 (dd, J = 2.8, 14.0 Hz, 1 H), 1.54–1.40 (m, 3 H), 1.37–1.18 (m, 3 H), 0.98 (d, J = 6.9 Hz, 3 H), 0.94 (t, J = 7.9 Hz, 3 H), 0.79 (s, 3 H); ^{13}C NMR (75 MHz, C_6D_6) (ppm) 151.28, 149.60, 124.61, 108.43, 73.31, 55.67, 49.68, 47.66, 41.45, 39.76, 36.68, 31.79, 31.43, 27.64, 27.23, 23.13, 22.60, 12.03; MS m/z (M^+) calcd 260.2140, obsd 260.2145.

Anal. Calcd for $C_{18}H_{28}O$: C, 83.02; H, 10.84. Found: C, 82.81; H, 10.94.

Addition of 15 to 7. Following the condensation of **15** with **7** under standard conditions, MPLC afforded 25 mg (10%) of **18A** and 210 mg (81%) of **18B**.

For **18A**: colorless oil; IR (neat, cm^{-1}) 3460, 2940, 2920, 2860, 1450, 1370, 1015, 970, 875; ^1H NMR (300 MHz, C_6D_6) δ 5.52 (s, 1 H), 4.74 (m, 1 H), 4.63 (m, 1 H), 2.54 (ddt, J = 2.0, 7.3, 16.4 Hz, 1 H), 2.23 (m, 1 H), 2.16 (m, 2 H), 2.02 (m, 1 H), 1.90 (m, 1 H), 1.83–1.65 (m, 3 H), 1.59–1.40 (m, 4 H), 1.08 (s, 1 H), 0.99 (d, J = 7.2 Hz, 3 H), 0.98 (t, J = 7.5 Hz, 3 H), 0.84 (s, 3 H); ^{13}C NMR (75 MHz, C_6D_6) (ppm) 154.04, 149.25, 124.54, 101.15, 78.31, 55.15, 46.82, 39.33, 39.15, 37.50, 35.56, 27.79, 27.16, 25.15, 24.48, 23.93, 22.77, 12.18; MS m/z (M^+) calcd 258.1984, obsd 258.1980.

For **18B**: colorless oil; IR (neat, cm^{-1}) 3470, 2840, 2820, 2760, 1660, 1450, 1050, 1020, 860; ^1H NMR (300 MHz, C_6D_6) δ 5.45 (s, 1 H), 4.78 (m, 1 H), 4.67 (s, 1 H), 2.55 (ddt, J = 2.2, 7.9, 16.4 Hz, 1 H), 2.46 (m, 1 H), 2.29 (m, 1 H), 2.19 (m, 1 H), 1.99 (m, 1 H), 1.91–1.67 (series of m, 3 H), 1.60 (d, J = 5.7 Hz, 1 H), 1.55 (m, 1 H), 1.51 (d, J = 5.7 Hz, 1 H), 1.38 (m, 2 H), 1.12 (s, 1 H), 1.04 (d, J = 7.0 Hz, 3 H), 0.94 (d, J = 7.4 Hz, 3 H), 0.83 (s, 3 H); ^{13}C NMR (75 MHz, C_6D_6) (ppm) 154.12, 149.66, 124.11, 101.31, 78.36, 55.37, 48.27, 39.94, 39.36, 36.98, 35.87, 27.58, 27.27, 25.37, 24.40, 23.88, 23.21, 11.81; MS m/z (M^+) calcd 258.1984, obsd 258.1978.

Anal. Calcd for $C_{18}H_{26}O$: C, 83.67; H, 10.14. Found: C, 83.44; H, 10.18.

Addition of 20 to 6. Reaction of **20** with **6** at the usual 1.0-mmol level afforded 30 mg (12%) of **21A**, 65 mg (25%) of **21C**, 17 mg (7%) of **21B**, and 103 mg (40%) of **21D**.

For **21A**: colorless liquid; IR (neat, cm^{-1}) 3500, 2930, 2850, 1460, 1440, 1060, 1010, 870; ^1H NMR (300 MHz, C_6D_6) δ 5.41 (s, 1 H), 4.91 (m, 1 H), 4.82 (m, 1 H), 3.05 (m, 1 H), 2.68 (m, 1 H), 2.52 (ddd, J = 2.3, 9.7, 16.9 Hz, 1 H), 2.29 (m, 1 H), 2.12–1.82 (m, 6 H), 1.81 (m, 1 H), 1.74 (m, 1 H), 1.65 (m, 1 H), 1.62–1.25 (m, 5 H), 1.08 (m, 2 H), 0.75 (s, 3 H); ^{13}C NMR (75 MHz, C_6D_6) (ppm) 150.30, 148.42, 125.92, 110.18, 73.16, 51.12, 49.62, 46.47, 42.58, 41.32, 39.88, 35.48, 34.37, 31.74, 31.33, 27.45, 27.14, 22.97; MS m/z (M^+) calcd 258.1984, obsd 258.1961.

For **21B**: colorless liquid; IR (neat, cm^{-1}) 3450, 2930, 2850, 1440, 1035, 1010, 970, 875; ^1H NMR (300 MHz, C_6D_6) δ 5.35 (m, 1 H), 4.82 (m, 1 H), 4.71 (m, 1 H), 3.20 (m, 1 H), 2.64 (m, 1 H), 2.56 (m, 1 H), 2.42 (m, 2 H), 1.94 (m, 2 H), 1.89 (m, 2 H), 1.78 (m, 3 H), 1.59 (m, 1 H), 1.48 (m, 3 H), 1.38 (dd, J = 13.9, 2.7 Hz, 1 H), 1.25 (m, 2 H), 0.93 (s, 1 H), 0.79 (s, 3 H); ^{13}C NMR (75 MHz, C_6D_6) (ppm) 152.14, 149.25, 125.05, 73.47, 50.58, 49.98, 46.35, 42.40, 40.95, 39.73, 35.43, 34.07, 32.31, 27.65, 27.23, 22.29; MS m/z (M^+) calcd 258.1984, obsd 258.1944.

For **21C**: colorless liquid; IR (neat, cm^{-1}) 3460, 2940, 2860, 1460, 1450, 1440, 1060, 1010, 880; ^1H NMR (300 MHz, C_6D_6) δ 5.28 (m, 1 H), 4.90 (m, 1 H), 4.83 (m, 1 H), 3.34 (m, 1 H), 2.64 (m, 1 H), 2.56 (m, 1 H), 2.35 (m, 1 H), 2.13 (m, 1 H), 1.95 (m, 2 H), 1.80 (m, 4 H), 1.71 (m, 1 H), 1.62 (m, 1 H), 1.58 (s, 1 H), 1.49 (m, 3 H), 1.44 (m, 1 H), 1.29 (m, 2 H), 0.77 (s, 3 H); ^{13}C NMR (75 MHz, C_6D_6) (ppm) 150.35, 148.80, 124.83, 109.64, 73.17, 51.46, 49.55, 47.43, 41.93, 41.18, 40.32, 35.65, 33.36, 32.37, 31.26, 27.44, 27.03, 23.55; MS m/z (M^+) calcd 258.1984, obsd 258.1997.

For **21D**: colorless oil; IR (neat, cm^{-1}) 3450, 2940, 2860, 1450, 1010, 975, 875; ^1H NMR (300 MHz, C_6D_6) δ 5.33 (m, 1 H), 4.78 (m, 1 H), 4.73 (m, 1 H), 3.17 (m, 1 H), 2.57 (m, 1 H), 2.52 (m, 1 H), 2.37 (m, 2 H), 1.96 (m, 1 H), 1.92 (m, 1 H), 1.83 (m, 1 H), 1.77 (m, 2 H), 1.72 (m, 2 H), 1.66–1.39 (m, 5 H), 1.25 (m, 2 H), 0.88 (s, 1 H), 0.79 (s, 3 H); ^{13}C NMR (75 MHz, C_6D_6) (ppm) 151.55, 149.57, 125.01, 108.39, 73.63, 51.52, 49.61, 47.61, 41.73, 41.45, 40.35, 35.63, 33.27, 31.90, 31.45, 27.67, 26.86, 22.55; MS m/z (M^+) calcd 258.1984, obsd 258.2007.

Anal. Calcd for $C_{18}H_{26}O$: C, 83.66; H, 10.15. Found: C, 83.66; H, 10.14.

Addition of 22 to 6. The condensation of **22** with 1.0 mmol of **6** in the predescribed manner provided **23A** (15 mg, 6%), **23C** (37 mg, 15%), **23B** (41 mg, 17%), and **23D** (101 mg, 41%).

For **23A**: colorless oil; IR (neat, cm^{-1}) 3500, 2940, 2860, 2840, 1645, 1450, 1065, 1020, 900, 880; ^1H NMR (300 MHz, C_6D_6) δ 5.56 (s, 1 H), 4.83 (m, 1 H), 4.75 (m, 1 H), 3.37 (br s, 1 H), 2.77 (m, 1 H), 2.48 (m, 1 H), 2.40–2.26 (m, 3 H), 2.17–2.04 (m, 4 H), 1.96 (dm, J = 16.7 Hz, 1 H), 1.83 (dm, J = 16.8 Hz, 1 H), 1.76–1.72 (m, 1 H), 1.69 (dd, J = 2.9, 14.0 Hz, 1 H), 1.55–1.39 (m, 2 H), 1.42 (dd, J = 3.0, 14.0 Hz, 1 H), 1.22 (m, 1 H), 0.77 (s, 3 H); ^{13}C NMR (75 MHz, C_6D_6) (ppm) 151.23, 148.37, 126.56, 110.14, 73.92, 49.63, 46.57, 41.27, 40.57, 36.71, 31.79, 31.34, 29.25, 27.71, 27.41, 22.97; MS m/z ($M^+ - H_2O$) calcd 226.1722, obsd 226.1693.

For **23B**: colorless oil; IR (neat, cm^{-1}) 3460, 2960, 2930, 2830, 1450, 1055, 1015, 875; ^1H NMR (300 MHz, C_6D_6) δ 5.48 (s, 1 H), 4.75 (m, 1 H), 4.68 (m, 1 H), 3.36 (m, 1 H), 2.79 (m, 1 H), 2.51–2.29 (m, 3 H), 2.24 (t, J = 2.8 Hz, 1 H), 2.18–2.02 (m, 3 H), 1.97–1.65 (m, 4 H), 1.53–1.39 (m, 3 H), 1.27–1.14 (m, 2 H), 0.79 (s, 3 H); ^{13}C NMR (75 MHz, C_6D_6) (ppm) 152.90, 140.08, 125.90, 108.07, 74.15, 49.70, 46.72, 45.57, 41.00, 40.35, 36.60, 32.22, 31.39, 28.99, 27.57, 22.26; MS m/z ($M^+ - H_2O$) calcd 226.1722, obsd 226.1706.

For **23C**: colorless oil; IR (neat, cm^{-1}) 3460, 2940, 2860, 2830, 1650, 1460, 1055, 1015, 890, 880; ^1H NMR (300 MHz, C_6D_6) δ 5.55 (s, 1 H), 4.89 (m, 1 H), 4.82 (m, 1 H), 3.56 (br s, 1 H), 2.81 (m, 1 H), 2.51 (m, 1 H), 2.38–2.31 (m, 2 H), 2.17–2.04 (m, 4 H), 1.90 (dm, J = 16.6 Hz, 1 H), 1.82 (dm, J = 14.1 Hz, 1 H), 1.79–1.66 (m, 3 H), 1.53 (m, 1 H), 1.44 (dm, J = 14.2 Hz, 1 H), 1.12 (m, 2 H), 0.77 (s, 3 H); ^{13}C NMR (75 MHz, C_6D_6) (ppm) 151.20, 148.64, 126.40, 109.80, 73.38, 49.05, 47.76, 46.11, 41.17, 40.67, 36.73, 32.28, 31.19, 28.41, 27.67, 27.42, 23.59; MS m/z ($M^+ - H_2O$) calcd 226.1722, obsd 226.1715.

For **23D**: colorless oil; IR (neat, cm^{-1}) 3460, 2940, 2860, 2830, 1650, 1460, 1450, 880; ^1H NMR (300 MHz, C_6D_6) δ 5.55 (s, 1 H), 4.86 (m, 1 H), 4.79 (m, 1 H), 3.33 (br s, 1 H), 2.84 (m, 1 H), 2.53–2.38 (m, 3 H), 2.21–2.13 (m, 3 H), 2.06–1.90 (m, 3 H), 1.88–1.76 (m, 2 H), 1.58–1.37 (m, 3 H), 1.08 (m, 2 H), 0.75 (s, 3 H); ^{13}C NMR (75 MHz, C_6D_6) (ppm) 152.37, 149.60, 125.78, 108.36, 73.97, 49.58, 48.17, 46.50, 41.35, 40.51, 36.71, 31.85, 31.40, 28.62, 27.64, 27.45, 22.71; MS m/z ($M^+ - H_2O$) calcd 226.1722, obsd 226.1728.

Anal. Calcd for $C_{17}H_{24}O$: C, 83.55; H, 9.90. Found: C, 83.52; H, 9.90.

Addition of 20 to 7. In this instance, two alcohols were obtained: **26A** (56 mg, 22%) and **26B** (122 mg, 48%).

For **26A**: colorless liquid; IR (neat, cm^{-1}) 3460, 2940, 2860, 1650, 1445, 1085, 1050, 1020, 960, 860; ^1H NMR (300 MHz, C_6D_6) δ 5.48 (m, 1 H), 4.76 (m, 1 H), 4.67 (m, 1 H), 3.15 (m, 1 H), 2.26 (m, 1 H), 2.52 (m, 1 H), 2.30 (m, 1 H), 2.24 (m, 1 H), 1.96 (m, 1 H),

1.90–1.67 (series of m, 4 H), 1.66–1.51 (m, 4 H), 1.46 (m, 2 H), 1.28 (m, 2 H), 0.86 (s, 3 H); ^{13}C NMR (75 MHz, C_6D_6) (ppm) 154.17, 150.38, 124.92, 101.12, 78.29, 50.90, 47.28, 42.22, 39.99, 39.52, 35.63, 35.43, 34.10, 27.91, 27.04, 25.48, 24.51, 24.00; MS m/z (M^+) calcd 256.1828, obsd 256.1812.

For **26B**: colorless liquid; IR (neat, cm^{-1}) 3450, 2940, 2860, 1655, 1445, 1050, 1025, 960, 860; ^{1}H NMR (300 MHz, C_6D_6) δ 5.42 (m, 1 H), 4.77 (s, 1 H), 4.66 (s, 1 H), 3.28 (m, 1 H), 2.63 (m, 1 H), 2.55 (m, 1 H), 2.27 (m, 1 H), 2.20 (m, 1 H), 1.97 (m, 1 H), 1.93–1.80 (m, 1 H), 1.78–1.68 (m, 3 H), 1.76 (d, J = 5.9 Hz, 1 H), 1.63–1.59 (m, 4 H), 1.55 (d, J = 5.9 Hz, 1 H), 1.29 (m, 1 H), 1.15 (m, 1 H), 0.85 (s, 3 H); ^{13}C NMR (75 MHz, C_6D_6) (ppm) 154.25, 150.12, 124.53, 101.12, 78.58, 51.26, 48.31, 41.95, 40.28, 39.12, 35.97, 35.66, 33.47, 27.67, 26.83, 25.54, 24.44, 23.98; MS (m/z) (M^+) calcd 256.1828, obsd 256.1822.

Anal. Calcd for $C_{18}H_{24}O$: C, 84.32; H, 9.44. Found: C, 84.12; H, 9.53.

Addition of 22 to 7. Reaction of **22** with 1.0 mmol of **7** as predescribed furnished 59 mg (24%) of **27A** and 127 mg (53%) of **27B**.

For **27A**: colorless liquid; IR (neat, cm^{-1}) 3430, 2920, 2840, 1650, 1080, 1050, 1015; ^{1}H NMR (300 MHz, C_6D_6) δ 5.63 (s, 1 H), 4.75 (s, 1 H), 4.63 (s, 1 H), 3.38 (br s, 1 H), 2.80 (m, 1 H), 2.50 (m, 1 H), 2.37 (m, 1 H), 2.23–2.04 (series of m, 6 H), 1.86 (m, 2 H), 1.74 (m, 2 H), 1.62–1.48 (m, 2 H), 0.85 (s, 3 H); ^{13}C NMR (75 MHz, C_6D_6) (ppm) 153.93, 151.21, 125.48, 101.18, 78.94, 47.32, 45.90, 40.58, 39.35, 36.58, 35.72, 29.27, 27.66, 25.53, 24.43, 23.96; MS m/z (M^+) calcd 242.1670, obsd 242.1632.

For **27B**: colorless liquid; IR (neat, cm^{-1}) 3420, 2930, 2900, 2850, 2830, 1660, 1450, 1430, 1095, 1065, 1050, 1030, 960, 905, 860; ^{1}H NMR (300 MHz, C_6D_6) δ 5.68 (s, 1 H), 4.78 (s, 1 H), 4.67 (s, 1 H), 3.46 (br s, 1 H), 2.80 (m, 1 H), 2.49 (m, 1 H), 2.35 (m, 1 H), 2.26 (m, 1 H), 2.23–2.02 (m, 4 H), 1.87 (m, 2 H), 1.73 (m, 2 H), 1.61 (d, J = 5.7 Hz, 1 H), 1.52 (d, J = 5.7 Hz, 1 H), 1.50 (m, 1 H), 0.84 (s, 3 H); ^{13}C NMR (75 MHz, C_6D_6) (ppm) 154.38, 151.58, 125.28, 101.08, 78.68, 48.16, 46.15, 40.44, 38.78, 36.70, 35.82, 28.78, 27.57, 25.74, 24.42, 23.93; MS m/z (M^+) calcd 242.1670, obsd 242.1663.

Anal. Calcd for $C_{17}H_{22}O$: C, 84.24; H, 9.15. Found: C, 84.19; H, 9.07.

Prototypical Anionic Oxy-Cope Rearrangement Procedure. Isomerization of 11D. A solution of 0.5 mmol of **11D** in 15 mL of dry tetrahydrofuran was treated with a 0.5 M toluene solution of potassium hexamethyldisilazide (0.7 mmol) and refluxed under a nitrogen atmosphere for 2 h until the conversion was complete as judged by TLC analysis. The cooled reaction mixture was treated with saturated ammonium chloride solution, and the product ketone was extracted into ether (3 × 10 mL). The combined organic phases were washed with brine (2 × 10 mL), dried, and evaporated. MPLC purification (silica gel, elution with 5% ether in petroleum ether) afforded **12** (18 mg, 50%) as a colorless crystalline solid: mp 68–70 °C (from methanol); IR (KBr, cm^{-1}) 2940, 2910, 2850, 1680, 1450, 1440, 1370, 1180, 1150, 1080; ^{1}H NMR (300 MHz, C_6D_6) δ 5.37 (m, 1 H), 2.81 (br s, 1 H), 2.28 (br s, 1 H), 2.24 (br s, 1 H), 2.07–2.04 (m, 5 H), 1.94–1.81 (m, 4 H), 1.78–1.62 (m, 3 H), 1.55 (m, 1 H), 1.51 (m, 1 H), 1.23 (m, 1 H), 0.84 (d, J = 6.5 Hz, 3 H), 0.82 (s, 3 H), 0.76 (d, J = 6.5 Hz, 3 H); ^{13}C NMR (75 MHz, C_6D_6) (ppm) 126.17, 60.41, 55.92, 55.01, 48.46, 42.38, 37.90, 36.97, 34.76, 32.55, 30.03, 29.76, 28.37, 23.66, 23.19, 22.13; MS m/z (M^+) calcd 260.2140, obsd 260.2145; X-ray analysis, see below.

Isomerization of 13B. A reaction time of 65 h was required to achieve completion of the rearrangement; **14** was isolated in 66% yield (91 mg): colorless crystals, mp 110–112 °C (from methanol); IR (KBr, cm^{-1}) 2950, 2900, 2860, 2840, 1680, 1100; ^{1}H NMR (300 MHz, C_6D_6) δ 5.54 (m, 1 H), 2.71 (m, 1 H), 2.64 (dd, J = 4.9, 13 Hz, 1 H), 2.24 (m, 1 H), 2.20 (m, 1 H), 2.01 (m, 1 H), 1.89 (m, 1 H), 1.83 (m, 1 H), 1.77 (m, 1 H), 1.62 (m, 1 H), 1.56 (dd, J = 6.5, 12 Hz, 1 H), 1.48 (m, 1 H), 1.43 (d, J = 10 Hz, 1 H), 1.38 (m, 2 H), 1.32 (dd, J = 4.7, 10 Hz, 1 H), 0.91 (d, J = 6.6 Hz, 3 H), 0.90 (s, 3 H), 0.83 (d, J = 6.6 Hz, 4 H); ^{13}C NMR (75 MHz, C_6D_6) (ppm) 204.79, 134.06, 128.78, 58.18, 53.49, 42.55, 41.51, 36.77, 29.24, 28.51, 27.26, 26.91, 26.47, 25.16, 25.04, 23.62, 22.85, 22.26; MS m/z (M^+) calcd 258.1984, obsd 258.1988; X-ray analysis, see below.

Isomerization of 16D. A total heating time of 12 h was required, and **17** was isolated in 56% yield (28 mg): colorless crystals, mp 52–53 °C (from methanol); IR (KBr, cm^{-1}) 2940, 2920, 2860, 1680, 1450; ^{1}H NMR (300 MHz, C_6D_6) δ 5.35 (m, 1 H), 2.76 (m, 1 H), 2.34–2.13 (m, 5 H), 2.10–1.84 (m, 6 H), 1.73 (m, 1 H), 1.56 (m, 1 H), 1.42–1.21 (m, 3 H), 1.14 (m, 1 H), 0.99 (d, J = 6.6 Hz, 3 H), 0.83 (s, 3 H), 0.82 (t, J = 7.2 Hz, 3 H); ^{13}C NMR (20 MHz, C_6D_6) (ppm) 212.22, 136.44, 126.49, 59.52, 57.15, 56.50, 44.98, 41.94, 39.24, 37.86, 37.53, 36.73, 32.40, 23.54, 22.78, 14.12; MS m/z (M^+) calcd 260.2140, obsd 260.2148; X-ray analysis, see below.

Isomerization of 18B. After a reaction time of 12 h, there was isolated 153 mg (85%) of **19**: colorless crystalline solid, mp 90–91 °C (from methanol); IR (KBr, cm^{-1}) 2970, 2940, 2900, 2860, 1690, 1455, 1440, 1410, 1110, 1095; ^{1}H NMR (300 MHz, C_6D_6) δ 5.53 (m, 1 H), 2.74 (t, J = 5.4 Hz, 1 H), 2.65 (dd, J = 4.9, 13.3 Hz, 1 H), 2.41–2.17 (m, 2 H), 2.12–1.78 (m, 4 H), 1.66 (m, 1 H), 1.51 (m, 2 H), 1.40 (d, J = 10.2 Hz, 1 H), 1.22 (m, 3 H), 0.99 (d, J = 6.9 Hz, 3 H), 0.92 (m, 1 H), 0.90 (s, 3 H), 0.85 (t, J = 7.5 Hz, 3 H); ^{13}C NMR (75 MHz, C_6D_6) (ppm) 204.44, 134.10, 128.68, 59.11, 55.45, 41.33, 40.24, 36.71, 36.63, 36.42, 26.89, 26.50, 24.98, 23.61, 22.77, 22.38; MS m/z (M^+) calcd 258.1984, obsd 258.1960.

Anal. Calcd for $C_{18}H_{26}O$: C, 83.67; H, 10.14. Found: C, 83.69; H, 10.11.

Isomerization of 21D. After a 12-h reaction time, 44 mg (50%) of **24** was isolated: colorless crystalline solid, mp 65–67 °C (from methanol); IR (KBr, cm^{-1}) 2940, 2920, 2900, 2860, 2840, 2820, 1670, 1450; ^{1}H NMR (300 MHz, C_6D_6) δ 5.34 (m, 1 H), 2.34 (m, 2 H), 2.18 (m, 1 H), 2.08–2.01 (m, 2 H), 1.99–1.80 (m, 4 H), 1.72 (m, 1 H), 1.61 (m, 3 H), 1.51–1.21 (series of m, 7 H), 0.95 (s, 3 H), 0.85 (m, 1 H), 0.68 (m, 1 H); ^{13}C NMR (75 MHz, C_6D_6) (ppm) 211.92, 139.65, 125.11, 67.00, 51.36, 47.51, 44.90, 42.90, 41.65, 40.96, 40.01, 38.35, 33.59, 32.23, 31.87, 31.35, 24.86, 22.75; MS m/z (M^+) calcd 258.1984, obsd 258.1986.

Anal. Calcd for $C_{18}H_{26}O$: C, 83.66; H, 10.15. Found: C, 83.37; H, 10.05.

Isomerization of 23D. After a 12-h reaction period, 108 mg (60%) of **25** was isolated: colorless oil; IR (neat, cm^{-1}) 2920, 2850, 1680, 1450; ^{1}H NMR (300 MHz, C_6D_6) δ 5.38 (m, 1 H), 2.63 (m, 2 H), 2.46 (dd, J = 11.1, 6.5 Hz, 1 H), 2.28 (m, 1 H), 2.23–2.03 (series of m, 4 H), 1.95 (m, 2 H), 1.82 (m, 3 H), 1.64 (m, 1 H), 1.55 (m, 3 H), 1.28–1.11 (m, 3 H), 1.04 (s, 3 H); ^{13}C NMR (75 MHz, C_6D_6) (ppm) 213.13, 139.21, 124.23, 67.99, 50.91, 49.10, 43.73, 42.24, 41.90, 39.40, 39.12, 37.84, 33.09, 30.63, 26.73, 26.21, 22.88; MS m/z (M^+) calcd 244.1827, obsd 244.1820.

Anal. Calcd for $C_{17}H_{24}O$: C, 83.55; H, 9.90. Found: C, 83.42; H, 9.89.

Isomerization of 26B. After a heating period of 12 h, there was isolated 74 mg (62%) of **28**: colorless crystalline solid, mp 74–75 °C (from methanol); IR (KBr, cm^{-1}) 2980, 2930, 2850, 1680, 1450, 1440, 835; ^{1}H NMR (300 MHz, C_6D_6) δ 5.55 (m, 1 H), 2.51 (m, 1 H), 2.32 (m, 3 H), 1.99–1.93 (m, 2 H), 1.86 (m, 1 H), 1.79 (m, 1 H), 1.73–1.60 (m, 4 H), 1.57 (m, 1 H), 1.50–1.37 (m, 4 H), 1.27 (m, 1 H), 0.98 (s, 3 H), 0.85 (m, 1 H), 0.65 (m, 1 H); ^{13}C NMR (75 MHz, C_6D_6) (ppm) 210.21, 138.40, 126.87, 63.92, 47.58, 42.58, 41.91, 40.93, 40.66, 40.33, 33.58, 33.51, 28.53, 26.77, 24.67, 23.99, 23.09, 20.70; MS m/z (M^+) calcd 256.1828, obsd 256.1831.

Anal. Calcd for $C_{18}H_{24}O$: C, 84.32; H, 9.44. Found: C, 84.05; H, 9.39.

Isomerization of 27B. Heating **27B** for 12 h gave rise to 189 mg (59%) of **29**: colorless solid, mp 108–110 °C (from methanol); IR (KBr, cm^{-1}) 2930, 2880, 2830, 2800, 1690, 1460, 1450, 1120, 1090; ^{1}H NMR (300 MHz, C_6D_6) δ 5.69 (m, 1 H), 3.05 (m, 1 H), 2.79 (m, 1 H), 2.57 (m, 2 H), 2.48 (m, 2 H), 2.30 (m, 2 H), 1.95–1.74 (m, 3 H), 1.69–1.40 (m, 6 H), 0.98 (m, 1 H), 0.95 (s, 3 H); ^{13}C NMR (75 MHz, C_6D_6) (ppm) 204.64, 136.99, 127.41, 63.21, 40.73, 40.69, 39.09, 39.02, 38.92, 37.60, 26.71, 26.65, 26.39, 24.04, 23.22, 22.33, 21.84; MS m/z (M^+) calcd 242.1670, obsd 242.1675; X-ray analysis, see Figure 5 and supplementary material.

X-ray Crystallographic Analysis of 12. A transparent single crystal of **14** was mounted on a pin and transferred to a goniometer. The space group was determined to be the centric $P2_1/n$ from the systematic absences. A summary of data-collection parameters is given in Table III. Least-squares refinement with isotropic thermal parameters led to R = 0.144. Those hydrogen atoms geometrically constrained were placed in calculated positions 0.95 Å from the bonded carbon atom and allowed to ride on that atom with B fixed at 5.5 Å^2. The remaining hydrogen atoms were located from a difference Fourier map and included

with fixed contributions (B = 5.5 Å^2). Refinement of the non-hydrogen atoms with anisotropic temperature factors led to final values of R = 0.053 and R_w = 0.055. The final values of the positional parameters are given in the supplementary material.

X-ray Crystallographic Analysis of 14. A transparent single crystal of the title complex was mounted on a pin and transferred to a goniometer. The space group was determined to be the centric $P2_1/c$ from the systematic absences. A summary of data-collection parameters is given in Table III. Least-squares refinement with isotropic thermal parameters led to R = 0.138. The geometrically constrained hydrogen atoms were placed in calculated positions 0.95 Å from the bonded carbon atom and allowed to ride on that atom with B fixed at 5.5 Å^2. The methyl hydrogen atoms were located from a difference Fourier map and included with fixed contributions (B = 5.5 Å^2). Refinement of the non-hydrogen atoms with anisotropic temperature factors led to final values of R = 0.054 and R_w = 0.057. The final values of the positional parameters are given in the supplementary material.

X-ray Crystallographic Analysis of 17. A transparent single crystal of the title complex was mounted on a pin and transferred to a goniometer. The space group was determined to be the centric $P2_1/c$ from the systematic absences. A summary of data-collection parameters is given in Table III. The geometrically constrained hydrogen atoms were placed in calculated positions 0.95 Å^2 from the bonded carbon atom and allowed to ride on that atom with B fixed at 5.5 Å^2. Least-squares refinement with isotropic thermal parameters led to R = 0.116. The methyl hydrogen atoms were located from a difference Fourier map and included with fixed contributions (B = 5.5 Å^2). Refinement of non-hydrogen atoms with anisotropic temperature factors led to the final values of R = 0.051 and R_w = 0.060. The final values of the positional parameters are given in the supplementary material.

Acknowledgment. We thank the National Institutes of Health for financial support (Grant GM-28468), Professor A. L. Rheingold for his efforts in solving the structure of **29** by X-ray crystallography, and George Maynard for his generous assistance with the MODEL calculations.

Supplementary Material Available: Tables of bond distances and angles, final fractional coordinates, thermal parameters, and least-squares planes for **12**, **14**, **17**, and (in part) **29** (17 pages); tables of observed and calculated structure factors for **12**, **14**, and **17** (10 pages). Ordering information is given on any current masthead page.

Dialdosides-(1,5) of Glucose and Galactose: Synthesis, Reactivity, and Conformation

Sujan Singh, Sudhir Nambiar, Richard A. Porter, Tony L. Sander, and K. Grant Taylor*

Department of Chemistry, University of Louisville, Louisville, Kentucky 40292

R. Jennings Doyle

Department of Microbiology and Immunology, University of Louisville, Louisville, Kentucky 40292

Received December 8, 1988

Methyl α-D-*gluco*-hexodialdoside-(1,5) 6-hydrate, **1a**, and the β-D-*gluco* (**4a**) and α-D-*galacto* (**6a**) isomers were prepared by oxidation of C6 by Moffatt, Swern, and photochemical oxidations. Dialdoside **1a** underwent dimer, hemiacetal, acetal, dithioacetal, and *gem*-diamine formation, exemplifying the facile transformations possible at C6, a strongly electrophilic aldehyde group. $NaBD_4$ reduction gave as predominant product the S diastereomer from **1a** and the R diastereomer from **6a**; reduction of **4a** gave almost equivalent amounts of R and S reduction product. These results were interpreted in terms of current theory of nucleophilic attack at chiral-substituted C=O groups. A combination of ^{1}H NMR spectroscopy, optical rotation data, and calculations was used to deduce the major C5–C6 rotamers of the dimethyl acetal of **1a** (06-R_{gg}), and of **4a** (06-R_{gg}) and **6a** (06-R_{gt}). NOE experiments supported the rotamer structure assignment for the dimethyl acetal.

The α-1,6- and α-1,3-linked glucans synthesized from sucrose by the exocellular glucosyltransferase enzymes (GTF) of oral bacteria are constituents of cariogenic plaque and are a virulence factor in the formation of smooth surface dental caries.[1,2] Studies of GTF and the oral bacteria *Streptococcus sanguis* and *Streptococcus mutans* suggest that inhibition of glucan synthesis should have a prophylactic effect on the cariogenic process.[2] Also, studies of inhibitors should help in mapping the active site(s) of the GTF enzymes. A number of carbohydrate derivatives have been made that are competitive or uncompetitive inhibitors.[2,3] We targeted aldehyde derivatives of sucrose and glucose as potential GTF inhibitors.[4] Herein, we report on the synthesis and chemistry of dialdosides of glucose and galactose.

Syntheses. Our targets were the water-soluble methyl dialdopyranoside hydrates **1a**, **4a**, and **6a**.[5] Pettersson and

(1) Gibbons, R. J.; vanHoute, J. In *Bacterial Adherence. Receptors and Recognition*; Beachy, E. H., Ed.; Chapman and Hall: London, 1980; pp 63–171.

(2) *Glucosyltransferases, Glucans, Sucrose and Dental Caries*; Doyle, R. J., Ciardi, J. E., Eds.; IRL Press: Washington, DC, 1983. This volume provides a general up-to-date review of the field.

(3) (a) Thaniyavarn, S.; Singh, S.; Maynard, C. M.; Taylor, K. G.; Doyle, R. J. *Carbohydr. Res.* **1981**, *96*, 134–37. (b) Binder, T. P.; Robyt, J. F. *Carbohydr. Res.* **1985**, *140*, 9–20 and references therein.

(4) (a) McAlister, D.; Singh, S.; Taylor, K. G.; Doyle, R. J. In *Molecular Microbiology and Immunobiology of Streptococcus mutans*; McGhee, J., Michalek, S., Hamada, S., Menaker, L., Eds.; Elsevier: Amsterdam, 1986; pp 413–19. (b) Doyle, R. J.; Nambiar, S.; Porter, R. A.; Sander, T. L.; Singh, S.; Taylor, K. G. *Abstracts of Papers*, 194th National Meeting of the American Chemical Society, New Orleans, LA; American Chemical Society, Washington, DC, 1987; CARB 23.

(5) Aldehydo forms of carbohydrates are extensively hydrated: (a) Fedoronko, M. *Collect. Czech., Chem. Commun.* **1984**, *49*, 1167–72. (b) Serianni, A. S.; Pierce, J.; Huang, S.-G.; Barker, R. *J. Am. Chem. Soc.* **1982**, *104*, 4037–44. (c) Angyal, S. J. *Adv. Carbohydr. Chem. Biochem.* **1984**, *42*, 15–68.

0022-3263/89/1954-2300$01.50/0